Journal of Colloid and Interface Science 390 (2013) 96–104

Contents lists available at SciVerse ScienceDirect

Journal of Colloid and Interface Science

www.elsevier.com/locate/jcis

Impact of diameter on carbon nanotube transport in sand

D.M. O'Carroll [a,*], X. Liu [b], N.T. Mattison [c], E.J. Petersen [d]

[a] Department of Civil & Environmental Engineering, The University of Western Ontario, London, ON, Canada N6A 5B8
[b] Water Infrastructure Management, Toronto Water, 55 John Street, Toronto, ON, Canada M5V 3C6
[c] Millennium EMS Solutions Ltd., Calgary, AB, Canada T2N 2A4
[d] Material Measurement Laboratory, National Institute of Standards and Technology, Gaithersburg, MD 20899, United States

ARTICLE INFO

Article history:
Received 3 August 2012
Accepted 17 September 2012
Available online 26 September 2012

Keywords:
Multiwall carbon nanotubes
Transport
Column experiments
Numerical modeling
Characterization
Size

ABSTRACT

Carbon nanotubes are the subject of intense research due to their unique properties: light weight, significant strength, excellent conductivity, and outstanding chemical resistance. This has led to their application in a wide variety of industries (e.g., in composite materials). As a result of their potential impact to humans and ecosystems, there is increasing interest in understanding the factors that control the transport of carbon nanotubes in the environment, and of particular interest to this study, their transport in porous media. In this work, the transport behavior of multiwall carbon nanotubes (MWCNTs) is investigated in sand packed column experiments. To determine the importance of MWCNT diameter, experiments were conducted using four commercially available MWCNTs. Results suggest that smaller MWCNTs are less mobile than their larger counterparts, likely due to the increase in Brownian motion leading to more MWCNT collisions with the porous media with decreasing MWCNT size. A numerical model was used to simulate observed MWCNT transport behavior and facilitate comparison with published studies. These results suggest that careful characterization of MWCNT characteristics (i.e., dimensions and initial MWCNT mass in suspension) is essential to adequately interpret observed results. Results from this study suggest that MWCNTs may be mobile under conditions expected in subsurface aquifers.

1. Introduction

Carbon nanotubes (CNTs) have been the subject of intense research in recent years. Their unique properties (e.g., light weight, significant strength, excellent conductivity, and outstanding chemical resistance) have led to their application in a wide variety of industries, such as in biomedical applications [1,2], construction [3] and environmental applications [4]. However, their ecotoxicological risks and potential human health risks after release into the environment are not yet well understood [5]. While substantial CNT uptake has not been observed in soil and sediment organisms [6–10], uptake up to 6.4% of the organism dry mass was observed in aquatic organism *Daphnia magna* and a food source was needed for nanotube elimination [11,12]. Furthermore, nanotube transport in subsurface ecosystems could lead to significant nanotube concentrations in groundwater which could be ingested by humans using drinking water wells. As such, it is critical to understand the factors that control the fate and transport of CNTs in the natural environment, and of particular interest to this study, their transport in porous media. An assessment of the mobility of carbon nanotubes in porous media would also facilitate predicting their removal rates by drinking water treatment facilities and their fate in subsurface aquifers.

A limited number of studies have investigated the transport of CNTs in porous media with many of these studies yielding differing results likely due to differing CNT properties (e.g., CNT type, dimensions, aspect ratio, stabilization methods) and experimental conditions (e.g., pore water velocity, mean grain size) [13–21]. These studies suggest that multiwall carbon nanotubes (MWCNTs) are less mobile at lower pore water velocities [16] and in finer porous media [17]. Additionally a single-wall carbon nanotube (SWCNT) transport study suggests that straining may be an important retention mechanism [15], but a recent MWCNT study suggests it was not [17]. No studies have investigated the impact of CNT dimensions on transport. Comparison of MWCNT and SWCNT transport, with SWCNTs having much smaller diameters, is unsatisfying in terms of an assessment of CNT dimension on transport as the intrinsic properties of these two CNT types are significantly different.

Traditional colloid filtration theory is widely used for the prediction of particle mobility in porous media systems. In the original development of this theory, the particles considered typically ranged in diameter from 1 to 100 μm. This theory yields model predictions that are in good agreement with experimental data when repulsive forces are absent between the particles and the collectors

* Corresponding author.
E-mail address: docarroll@eng.uwo.ca (D.M. O'Carroll).

0021-9797/$ - see front matter © 2012 Elsevier Inc. All rights reserved.
http://dx.doi.org/10.1016/j.jcis.2012.09.034

[22]. However, there is increasing evidence suggesting that discrepancies exist between theory and experimental data when the grain and particle are similarly charged (e.g., [18,23]). Researchers attributed this deviation from traditional filtration theory to a variety of factors including the role of secondary minimum deposition, surface charge heterogeneities of particles and collectors, and straining (e.g., [24,25]). Little research has focused on the utility of traditional colloid filtration theory to predict the mobility of nonspherical nanoparticles, such as carbon nanotubes. Two recent studies suggest that traditional colloid filtration theory can be used to simulate MWCNT transport with the inclusion of a site blocking term [16,17]. These studies suggest that there are a finite number of retention sites on porous media.

In this work, the impact of MWCNTs diameter on transport in porous media is investigated in sand packed column experiments. Experiments were conducted using commercially available MWCNTs with differing diameters. Furthermore the ability of a numerical model to reproduce observed transport behavior is assessed as well as the impact of initial MWCNT concentration on transport behavior.

2. Materials and methods

2.1. Multiwall carbon nanotubes

Multiwall carbon nanotubes (MWCNTs) were purchased from Cheap Tubes Inc. (Brattleboro, VT). These MWCNTs were synthesized using the chemical vapor deposition (CVD) method with metal catalysts. According to the manufacturer, energy dispersive X-ray spectroscopy revealed that these purified MWCNTs are over 97% by mass carbon. The manufacturer also provided MWCNT outer diameters and lengths by transmission electronic microscope (TEM) and Raman spectroscopy. Detailed dimension information is listed in Table 1.

Purchased carbon nanotubes were further functionalized using a concentrated aggressive acid mixture containing a 3 to 1 ratio by volume of sulfuric and nitric acids (95 to 97% and 70%, respectively) to enhance the MWCNT hydrophilicity through the addition of functional groups on the MWCNT surface [26]. Carbon nanotubes were mixed with these acids and sonicated for 2 h (AQUASONIC Ultrasonic Cleaner, VWR Scientific Products, West Chester, PA). Treated carbon nanotubes were filtered with a 0.45 mm polytetraflouroethylene (PTFE) filter membrane, then continuously rinsed with boiled de-ionized water until the aqueous phase was neutralized and finally dried in a vacuum desiccator. MWCNTs were still captured on the membrane as a result of their agglomeration despite many being smaller than 0.45 μm as discussed later.

This harsh modification process shortened SWCNTs at a rate of about 130 nm/h [26], but Petersen et al. [9] did not observe MWCNT shortening using this process, likely as a result of the multi-layer structure of MWCNTs inhibiting the shortening process. To analyze the size of the functionalized MWCNTs in this study, the nanotubes were suspended in de-ionized water using an ultrasonic probe (FISHER Sonic Dismembrator, ARTEK System Corporation, Farmingdale, NY) at 210 W for 45 min using an ice-water bath. A drop was then added to a holey carbon grid on a copper substrate (HC200-Cu, Electron Microscopy Sciences) and the sample allowed to dry. Two grids were prepared for each sample and a grid was also prepared with only water.

The MWCNTs were then analyzed using a ZEISS NVision 40 focused ion beam/scanning electron microscope (SEM) operating at 15 kV. To ensure comparable results among the different types of carbon nanotubes, the blank grid was analyzed and artifacts similar in shape to carbon nanotubes were not observed. Additionally, the same magnifications (25,000× for the length measurements and 75,000× for the diameter measurements) were used for all samples. There are several challenges associated with making size measurements using this method. To begin with, aggregation is a significant consideration in that it can hinder the identification of larger nanotubes by obscuring the nanotube ends. Similarly, smaller nanotubes could be concealed within aggregated clusters. Finally, it was sometimes difficult to differentiate between the smallest nanotubes and the sample grid. When the end of a nanotube could not be clearly determined, it was not used in the size counting performed manually using the program Digital Micrograph. Another limitation of this method was observed during SEM measurements of smaller MWCNT diameters, where the resolution at 75,000x made it difficult to identify nanotube edges. While the length and diameter distributions are believed to be representative of the samples, there is a need for additional research to improve measurement methods in determining carbon nanotube length and diameter distributions.

An ultrasonic probe was used to produce stable carbon nanotube suspensions in aqueous solutions at a pH of 10 and at two ionic strengths as described above. The first aqueous phase solution (SS I) had an ionic strength of 10 mmol/L and was buffered to pH 10 with 2.8 mmol/L $NaHCO_3$ and 2.1 mmol/L Na_2CO_3. One mmol/L NaBr or NaCl was added to SS I as a conservative tracer. For the low ionic strength aqueous phase solution (SS II) sodium hydroxide (NaOH) was added to de-ionized water to make a 0.1 mmol/L ionic strength solution with a pH around 10. An aqueous phase pH of 10 was selected to limit the impact of any sand impurities and ensure negative surface charge on both the MWCNTs and the sand. Two mg of carbon nanotubes were added to a 250 mL beaker containing 200 mL aqueous solution and sonicated. These suspensions were visually determined to be stable in the aqueous phase for months.

Concentrations of aqueous phase MWCNT suspensions were quantified using a ultraviolet–visible (UV–Vis) spectrophotometer (Cary 50, Varian, Australia) at a wavelength of 400 nm. An assessment of UV–Vis absorbance variability measured at six locations in the suspension beaker for MWCNT-a found that the coefficient of variation was 0.26%. Dilutions of the nominal 10 mg/L MWCNT suspension were used to develop an absorbance/concentration calibration curve.

2.2. Porous media

Quartz sand (d_{50} = 476 μm, U_I = 1.5; Barco 32, BEI Pecal, Hamilton, ON, CA) was used as the representative porous medium. Purchased quartz sand was cleaned alternately with hydrochloric

Table 1
Vendor reported and independently measured average multiwall carbon nanotube length and diameter (values in parentheses represent standard deviation).

	Vendor information		Independently measured	
	Outer diameter (nm)	Length (μm)	Outer diameter (nm)	Length (μm)
MWCNT-a	30–50	0.5–2.0	27.9 (8.6)	0.386 (0.264)
MWCNT-b	30–50	10–20	35.8 (10.6)	0.565 (0.364)
MWCNT-c	<8	0.5–2.0	9.5 (2.4)	0.236 (0.126)
MWCNT-d	<8	10–30	11.2 (3.4)	0.255 (0.143)

acid (0.1 mol/L) and hydrogen peroxide (5%) to remove all impurities and grease. De-ionized water was used to rinse the sand between steps and afterwards until a neutral pH was achieved. Washed sand was dried in an oven (105 °C) over night. Particles smaller than 152 μm were removed by sieving.

Aluminum columns, 5 cm in diameter and 10 cm in length, were dry packed with clean sand. A stainless steel mesh (150 μm openings) was placed at both ends of the column to support the sand as well as distribute the aqueous flow. The column was packed by adding sand in 0.5 cm lifts. Each lift was well mixed and tapped prior to adding subsequent lifts. Carbon dioxide gas was flushed through the column upwards for at least 15 min to displace air. De-ionized water was then pumped upwards through the column for at least 30 pore volumes to saturate the sand column. The weight difference between the unsaturated and water saturated column as well as the density of quartz sand (2.65 g/cm^3) were used to calculate the column pore volume. This packing procedure yielded an average column porosity and pore volume of 0.347 (ranging from 0.335 to 0.368) and 69.89 mL (ranging from 67.14 to 74.20 mL), respectively.

2.3. Column experiments

After saturating the column with de-ionized water the column was then flushed with flow vertically downwards for 10 pore volumes using the desired stock solution and then the flow rate was adjusted to the experimental flow condition (0.42 m/d or 4.86×10^{-6} m/s) for at least one pore volume before carbon nanotube injection. Dispersed MWCNTs were left undisturbed for at least 24 h to enable the solution to stabilize. 110 mL of the MWCNT suspensions were injected downwards through the column using a syringe pump and two 60 mL plastic syringes. 2.5 pore volumes of particle free solution, with the same solution chemistry, was then injected into the column at the same flowrate using a syringe pump. Effluent samples from the column were collected in 3.5 mL vials and the MWCNT concentration was determined using an UV–Vis spectrophotometer (Cary 50) at a wavelength of 400 nm. Conservative tracer concentrations (bromide or chloride) were quantified using high performance liquid chromatography (HPLC, Waters Company). Both MWCNT and tracer concentrations were used to generate breakthrough curves.

2.4. Mathematical model governing MWCNT transport

A one-dimensional finite element code was utilized to solve the aqueous and solid phases MWCNT mass balance equations [16] based on modified colloid filtration theory. The equation representing colloid or nanoparticle transport in the aqueous phase is represented as:

$$\frac{\partial C}{\partial t} + \frac{\rho_b}{n}\frac{\partial S}{\partial t} + v\frac{\partial C}{\partial x} - D\frac{\partial^2 C}{\partial x^2} = 0 \quad (1)$$

where C is the MWCNT concentration in the aqueous phase, t is time, ρ_b is the solid phase bulk density, n is porosity, S is the amount of carbon nanotubes associated with the solid phase, v is the pore water velocity, x is the spatial dimension in the column and D is the dispersion coefficient ($D = v^* \alpha_l$, where α_l is the longitudinal dispersivity).

For colloids or nanoparticles associated with the solid phase, the solid phase mass balance equation is represented as [27]:

$$\frac{\rho_b}{n}\frac{\partial S}{\partial t} - \left(\frac{3\alpha\eta_o v(1-n)}{2d_c}\right)\psi C + \frac{\rho_b k_{\mathrm{det}}}{n} S = 0 \quad (2)$$

where α is the attachment efficiency (i.e., number of MWCNTs that are retained on the sand collector divided by the number of MWCNTs that strike the sand collector), η_0 is the theoretical single collector efficiency (i.e., number of MWCNTs that strike the sand collector divided by the number of MWCNTs that approach the sand collector) and d_c is the mean diameter of the collector (grain), ψ is an absorption site blocking term and k_{det} is the rate constant for the detachment of MWCNTs associated with the solid phase. The adsorption site blocking term is further defined as:

$$\psi = \left(1 - \frac{S}{S_{\max}}\right) \quad (3)$$

where $S_{\max}$ is the maximum adsorption capacity of the solid phase for the removal of MWCNTs due to mechanisms typically associated with colloid filtration theory. Use of the absorption site blocking term implicitly assumes that only a finite number of MWCNT retention sites exist on the sand collector surface.

The attachment efficiency is typically fit to experimental data whereas the theoretical single collector efficiency can be calculated directly. Traditional colloid filtration theory assumes the theoretical single collector efficiency is the sum of the contact efficiencies due to interception (η_I), sedimentation (η_G) and diffusion (η_D) or:

$$\eta_0 = \eta_I + \eta_G + \eta_D \quad (4)$$

In this study, a theoretical single collector efficiency relationship specifically developed for non-spherical colloids (i.e., MWCNTs) in a spherical collector system was utilized due to the unique shape of the MWNTs [16]. This relationship was developed for two types of MWCNT/collector contact: the MWCNT end contacting the spherical collector (i.e., the circular end of the MWCNT contacting the spherical collector) and the MCWNT side contacting the collector (i.e., the length of the MWCNT contacting the spherical collector). Given the very small dimensions of the MWCNTs diffusion (η_D) dominates the theoretical single collector efficiency. As such both types of contact yield the same theoretical single collector efficiency. It is acknowledged that MWCNTs are not completely monodisperse and can also be present in the aqueous phase as aggregates or bundles. In addition MWCNTs are not rigid rods, as assumed in the development of the single collector efficiency relationship. However given that inadequate information exists regarding MWCNT morphology in the aqueous phase, the assumptions of monodisperse, rigid rods are implemented.

The numerical model has been validated through comparison to COMSOL V4.2 (Burlington, MA) simulations for identical input parameters. This numerical model has also been successfully employed for simulation of MWCNTs in two previous studies [16,17]. Known model parameters (e.g., pore water velocity, MWCNT dimensions, porosity) were input into the numerical model and unknown parameters (α, $S_{\max}$ and α_l) were fitted by minimizing the root mean square error (RMSE) between model and experimental MWCNT breakthrough. RMSE was minimized using a simplex search method [28]. These fitted model parameters (α, $S_{\max}$ and α_l) can be used for the simulation of MWCNT transport in field scale scenarios to facilitate risk analyses.

3. Results and discussion

3.1. Carbon nanotube characterization

Box plots of the lengths and diameters of the carbon nanotubes are shown in Fig. 1, and representative SEM micrographs used to assess the length and diameter distributions are shown in Figs. S1 and S2, respectively. As expected, the MWCNT diameters were quite similar between MWCNTs a and b and also between MWCNTs c and d. The average diameters were also near the ranges indicated by the manufacturer. Surprisingly, the lengths measured were much smaller than those indicated by the manufacturer, a

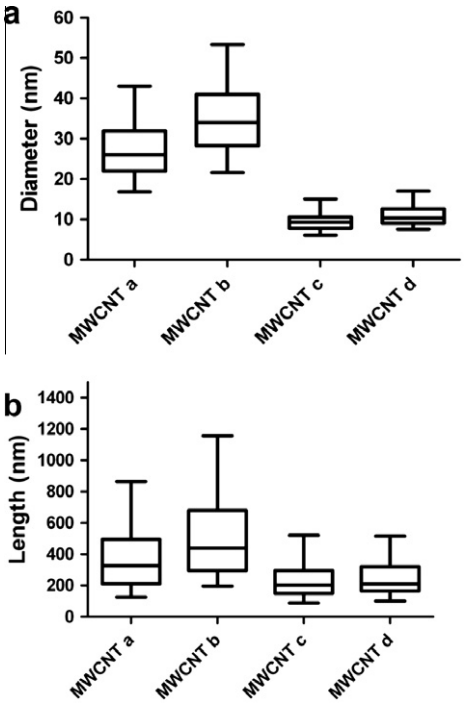

Fig. 1. Box plots of measured MWCNT diameter (a) and length (b). Whiskers represent the 5 and 95 percentiles, and the box represents one standard deviation. At least 200 and 130 samples were counted for length and diameter measurements, respectively.

result that may have stemmed from the acid washing procedure or sonication of the MWCNTs. Thus, the substantial difference in MWCNT length that had been expected among the different types of MWCNTs was not evident. MWCNTs a and b, which had larger diameters, did appear to be longer than the MWCNTs c and d overall, but there was not a clear difference between MWCNTs a and b or MWCNTs c and d. Part of this result may also stem from the likelihood that one large MWCNT could be broken down into multiple smaller MWCNTs which would then substantially decrease the average length.

3.2. Breakthrough curves of column experiments

A series of column experiments were conducted at 0.42 m/d (4.86×10^{-6} m/s) to assess the impact of MWCNT dimensions on transport. Breakthrough curves at low and high ionic strength are presented in Fig. 2. Normalized effluent concentration (i.e., effluent MWCNT concentration/injected MWCNT concentration) is plotted as a function of pore volumes (either MWCNT suspension or background solution) flushed through the column. Breakthrough curves of representative conservative tracer data (chloride and bromide) are also presented. Comparison of breakthrough curves for MWCNTs with differing dimensions, conducted at different ionic strength, to the conservative tracer results facilitates a determination of dominant transport and retention mechanisms. MWCNT-a exited the column at approximately the same time as the conservative tracer for the lower ionic strength solution and was retarded to a very small extent at the higher ionic strength solution (see Fig. 2). Similar breakthrough behavior for the low ionic strength solution experiments suggests that the experimental procedure yields reproducible results and that retention mechanisms that would be considered experimental artifacts are not operative. The maximum normalized effluent concentrations were similar at both ionic strengths (Fig. 2). MWCNT-b was retarded to a more significant extent at the higher ionic strength in comparison to MWCNT-a. Retardation behavior at the higher ionic strength was even more significant for MWCNT-c and MWCNT-d in comparison to MWCNT-a and MWCNT-b. It would appear that for the experiments conducted with the higher ionic strength solution a similar maximum effluent concentration to the lower ionic strength solution would be achieved if sufficient pore volumes were flushed. Unfortunately not enough pore volumes were flushed for MWCNT-c and d to verify this hypothesis. The column experiment results are consistent with colloid filtration theory (CFT) indicating that the lower ionic strength aqueous solution impeded MWCNT deposition on the porous medium [16,17,24,29]. At the higher ionic strength, steady-state effluent concentrations for MWCNT-a are larger than those of MWCNT-b and MWCNT-d. For these experiments it would appear that the smaller carbon nanotubes, both in terms of length and diameter (i.e., MWCNT-c and MWCNT-d have smaller diameters and lengths than MWCNT-a and MWCNT-b), are retained to a greater extent than the larger carbon nanotubes. The diameter of MWCNT-a is statistically larger than that of MWCNT-d and similar to that of MWCNT-b. Although the mean MWCNT length is longer for MWCNT-a and b, compared to MWCNT-c and d, they are not statistically different. The magnitude of Brownian motion for smaller MWCNTs (i.e., MWCNT-c and d) is greater than that of larger MWCNTs leading to more collisions with collectors as interception and sedimentation removal mechanisms are negligible under these conditions. Given the greater extent of Brownian motion and their smaller size it is possible that these smaller MWCNTs diffused into immobile zones (e.g., either into secondary pores if the sand had this structure or into zones with limited advective flow) leading to greater retention in the column. Differences in MWCNT surface properties causing differing transport behavior cannot be discounted; however all MWCNTs were treated using the same methodology and measured electrophoretic mobility values were all relatively large and negative (see Table 2). As such it is hypothesized that differences in MWCNT surface properties were small. In all cases, when the MWCNT injection ceased, effluent MWCNT concentrations rapidly decreased similar to the conservative tracer.

MWCNT-b results can be compared to those of a recent study by Mattison et al. [17] who used the same MWCNTs (i.e., same vendor and type; similar functionalization method), pore water velocity, and grain size as this study. Important differences between the two studies include pH and ionic strength: this study was conducted at pH = 10 and an ionic strength of 10 mmol/L, whereas the previous study was conducted at pH = 7.5 and an ionic strength of 7.5 mmol/L. Another important difference was the inlet concentration of MWCNTs to the column. In this study, the target initial concentration was 10 mg/L with an initial absorbance of 0.41 (Table 2). The Mattison et al. study had a target initial concentration of 8 mg/L with a reported initial absorbance of 0.239. The initial absorbance is a measure of the MWCNT concentration that remained in solution following sonication, with a higher initial absorbance indicating a higher initial mass concentration. Breakthrough of MWCNT-b in this study, at the high ionic strength, is significantly earlier than that of the study of Mattison et al. [17]. For example MWCNT-b attained a normalized effluent concentration of 0.7 at 2.3 pore volumes in this study whereas it took 5.6 pore volumes to achieve a normalized effluent concentration of 0.6 in their study. Differences in observed results are likely the result of differing initial concentrations in these experiments. Given that the initial concentration in the study of Mattison et al. [17] was lower, it would take more pore volumes of MWCNT suspension to fill MWCNT retention sites, delaying breakthrough. It is postulated here that the porous media has a limited number of retention sites for MWCNT removal. At higher initial concentrations, these retention sites would be filled more quickly. Initial

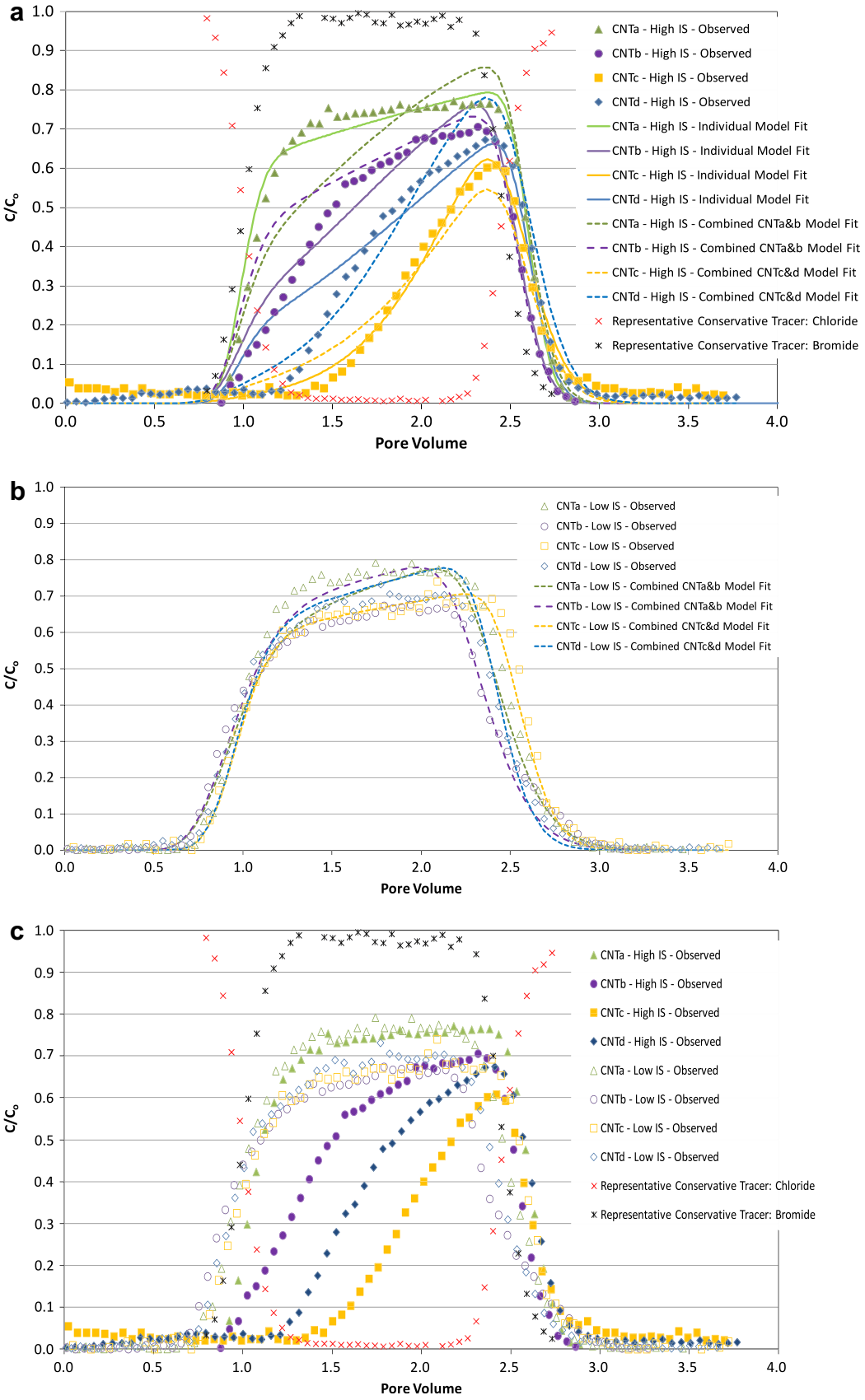

Fig. 2. Observed and model fitted breakthrough curves of MWCNTs at (a) high ionic strength (I = 10 mmol/L); (b) low ionic strength (I = 0.1 mmol/L); and (c) both low and high ionic strength. RMSE values provided in Tables 3 and 4 provide estimates of the quality of the modeling fits. The y-axis indicates the normalized concentration, and uncertainties for individual measurements can be approximated using the coefficient of variation value determined for the UV/Vis of 0.26%. Individual model fits indicate when only the data from that type of MWCNT was used in the fit, while the combined fits indicate when the data from both types of nanotubes was used to model the fit for that particular MWCNT.

Table 2
Summary of column experiment results.

MWCNT	Ionic strength (mmol/L)	Initial UV absorbance[a]	Measured electrophoretic mobility ($m^2/V/s$)[b]	Theoretical Single-collector efficiency (η_0)
a	10	0.60	−4.19 (0.17)	5.15×10^{-2}
	0.1	0.58	−3.61 (0.22)	5.15×10^{-2}
b	10	0.41	−3.53 (0.13)	1.16×10^{-2}
	0.1	0.58	−1.74 (0.25)	1.16×10^{-2}
c	10	0.35	−4.24 (0.25)	3.67×10^{-2}
	0.1	0.24	−3.84 (0.24)	3.67×10^{-2}
d	10	0.47	−5.20 (0.10)	8.09×10^{-3}
	0.1	0.45	−4.19*	8.09×10^{-3}

NA: Steady state not achieved.
[a] The coefficient of variation of six UV/Vis measurements was determined to be 0.26% in preliminary experiments.
[b] Information in parentheses denotes standard error.
* Standard error unavailable but assumed to similar to the other cases.

absorbance and mass loading to the column will also be discussed in the modeling section. This potentially highlights the importance of quantifying influent concentrations, although other experimental differences could also be important (e.g., pH and ionic strength).

Carbon nanotube removal is not solely related to collisions with collectors (η_0) but also related to the efficiency of these collisions (α) or the number of MWCNTs that are retained on the solid surface divided by the number of MWCNTs that strike the solid surface. Even though the surface functional groups of these carbon nanotubes should be similar, the differing carbon nanotube sizes could impact α. For example, larger carbon nanotubes may have more difficulty finding appropriate deposition sites as they will presumably need a larger area on the sand surface for deposition. Other factors that may influence α include the species and the concentrations of electrolyte in solution, pH, surface characteristics of MWCNTs, and the grain collectors [19].

In low ionic strength systems it is generally assumed that the energy barrier is too large for colloid removal due to deposition (i.e., interception, sedimentation, or Brownian diffusion). At the lower ionic strength, all of the carbon nanotubes generally exited the column with the conservative tracer. However, they all achieved a maximum normalized effluent concentration of less than 1.0, with MWCNT-a achieving a maximum normalized effluent concentration of 0.77 and the other carbon nanotubes achieving a maximum normalized effluent concentration of approximately 0.7. Given that deposition on the sand surface should be minimal at the lower ionic strength, other removal mechanisms are also important in carbon nanotube transport under these conditions. An important difference with the study of Mattison et al. [17] is that in their normalized effluent MWCNT concentrations approached 1.0, whereas in this study, the effluent concentration approached 0.7 at low ionic strength. The reason for this discrepancy is unclear as the only difference in experimental conditions in the Mattison et al. study [17] were pH and the constituents used to generate the pH buffer. It should be noted that normalized effluent concentrations were similar for all four low ionic strength experiments conducted in this study and for different grain sizes (three cases) in the Mattison et al. study [17].

3.3. Modeling MWCNT transport

A numerical model was used to model the transport of MWCNTs in the quartz sand packed columns. The unknown fitted parameters were attachment efficiency (α), maximum solid phase concentration (S_{max}), and dispersivity (α_l). Attachment of particles onto the sand grains was assumed to be permanent; thus, k_{det} was set to zero. This is consistent with experimental observations in this study as no tailing behavior was observed nor was tailing found in previous MWCNT transport studies [16,17]. A site blocking term (Eq. (3)), which included a maximum solid phase concentration, was used in the conceptual model as two recent MWCNT transport studies suggest that inclusion of this term is required to model the delayed MWCNT breakthrough observed experimentally for MWCNT-b, c and d [16,17]. These studies found that quartz sand has only a finite number of retention sites available for MWCNT retention. For the high ionic strength cases, two modeling approaches were adopted. The first approach fit unique unknown parameters to each MWCNT breakthrough experiment. In the second approach, a global fitting approach, unknown parameters were assumed to be the same for MWCNT-a and b and for MWCNT-c and d as these groups of MWCNTs had statistically equivalent dimensions. In addition the second approach assumed that initial UV absorbance for each experiment had a linear relationship with injected MWCNT mass, as will be discussed.

At high ionic strength, model fits using the first approach (i.e., individual model fit) are generally in good agreement with experimental results, especially for MWCNT-a and MWCNT-c. For MWCNT-b and d, model fits suggest that MWCNTs should exit the column before what was observed experimentally. In all cases, the maximum fitted effluent concentration immediately prior to cessation of the MWCNT injection was similar to experimental observations. Fitted attachment efficiencies do not follow a discernible trend; however, it is noteworthy that the attachment efficiency is greatest for the smallest MWCNT (Table 3). Maximum solid phase concentrations (S_{max}) are in a similar range with larger fitted values associated with the smaller diameter MWCNTs (Table 3). It is possible that the smaller MWCNTs are able to fit into a larger range of retention sites leading to a larger S_{max}. Given that the initial UV absorbance was different for each MWCNT, it is possible that injected MWCNT mass was not the same for each experiment (i.e., an identical MWCNT dispersion process did not result in the same MWCNT concentration for each MWCNT type). As noted in the Materials and Methods section UV–Vis absorbance was quantified at six different locations in the MWCNT-a suspension beaker and the coefficient of variation was 0.26% suggesting that the suspension was uniform and the UV/Vis measurements were precise. S_{max} is a measure of the total available sites for MWCNT deposition. With reduced MWCNT mass injected to the column, as suggested by some absorbance measurements, it would take longer to reach the capacity of the total available sites (S_{max}). The product of S_{max} and the initial MWCNTs UV absorbance can be used to correct for different initial UV absorbances (UV_o) as UV_o would account for the different MWCNT mass loading. This analysis assumes that initial MWCNTs UV absorbance can be directly compared between different MWCNT types (i.e., differences in UV absorbance is not a function of MWCNT geometry). This is considered reasonable given that the same instrument was used to quantify absorbance, the MWCNTs were synthesized using the

Table 3
Summary of model parameters and fits to each individual 10 mmol/L ionic strength experiment.

MWCNT	Attachment efficiency (α)	Maximum solid phase concentration (S_{max}) (μg/g)	Dispersivity (α_1) (m)	RMSE*
A	4.52×10^{-2}	1.55	4.74×10^{-4}	6.02×10^{-2}
B	1.61×10^{-1}	1.62	7.68×10^{-4}	4.80×10^{-2}
C	2.81×10^{-1}	2.47	1.50×10^{-3}	2.77×10^{-2}
D	1.11×10^{-1}	2.22	6.15×10^{-4}	6.37×10^{-2}

* Root mean square error determined by comparing model and experimental observations.

same process by the same supplier, and that solutions were prepared in the same manner. $S_{max} \times UV_o$ were 0.93, 0.66, 0.87 and 1.04 μg/g for MWCNT-a, b, c and d, respectively. The standard deviation of these initial UV absorbance adjusted S_{max} values is 18% with no discernible trend with MWCNT dimensions. A suite of simulations were conducted to explore the impact of initial injected MWCNT concentration on MWCNT breakthrough (Fig. 3). In these simulations, all MWCNTs were assumed to have the same initial injected MWCNT concentration, that of MWCNT-a. In these simulations, breakthrough of MWCNT-b, MWNCT-c and MWCNT-d occurs before that observed experimentally as the initial injected MWCNT concentration is larger (i.e., injected MWCNT-b, MWNCT-c and MWCNT-d concentrations increased by 46%, 71% and 28%, respectively, scaled to the initial absorbance of MWCNT-a). Even taking into account initial concentration differences, larger MWCNTs (MWCNT-a and MWCNT-b) were more mobile than the smaller MWCNTs (MWCNT-c and MWCNT-d), consistent with experimental observations. This sensitivity analysis highlights the importance of carefully quantifying initial MWCNT concentrations as it has a significant impact on MWCNT breakthrough. This analysis also highlights the importance of numerical modeling in interpretation of observed results as it would not have been straightforward to distill the importance of injected MWCNT concentration on observed effluent behavior. S_{max} fitted in the study of Mattison et al. [17] for MWCNT-b was larger (3.62 μg/g) than that fitted here. However, when their S_{max} is normalized to their initial UV absorbance and the different target MWCNT injection concentrations in the two studies are accounted for, the adjusted S_{max} is 0.69 μg/g, which is nearly identical to that in this study. Again, it is assumed that direct comparison of initial absorbances is reasonable for the reasons discussed above.

The second parameter fitting approach for the high ionic strength experiments took into account different initial absorbances by assuming the injected MWCNT mass was a linear function of the initial absorbance. As such this second parameter fitting approach can be considered a global fitting approach. Given that the dimensions of MWCNT-a and b and MWCNT-c and d were statistically equivalent, the same model parameter set was fitted to each MWCNT pair. In this case, model fits were not as good as the first approach since there were fewer degrees of freedom in the fitting routine (Fig. 2a). This is particularly apparent for MWCNT-a and b. The attachment efficiency (α) and maximum solid phase concentration (S_{max}) were larger for the smaller MWCNTs (MWCNT-c and d) suggesting that more collisions with the collector result in retention and that there are more retention sites available for the smaller MWCNTs (Table 4). As discussed above smaller MWCNTs may be able to fit into a wider range of retention sites.

Given that MWCNT pairs MWCNT-a and b and MWCNT-c and d were statistically equivalent and that the global fitting approach achieved reasonably good fits, this approach was adopted for the low ionic strength experiments. Due to the larger electrostatic energy barrier at the lower ionic strength, there were fewer retention sites in the lower ionic strength experiments in comparison to the higher ionic strength experiments. For this reason, the upper bound of the fitted S_{max} search area at the lower ionic strength was constrained at S_{max} fitted for the high ionic strength experiments, consistent with previous MWCNT transport studies [16]. The attachment efficiency was not constrained in this way as more collisions could result in attachment on this smaller subset of attachment sites. Model fits were generally in good agreement with experimental observations for the low ionic strength experiments, suggesting that this modeling approach is appropriate. Fitted attachment efficiencies were smaller than those fitted to the high ionic strength experiments and fitted S_{max} values were similar to those fitted to the high ionic strength experiments (Table 4). The fitted attachment efficiencies are consistent with behavior expected based on CFT due to the significant energy barrier to MWCNT deposition resulting in less deposition at the low ionic strength. Given that there is significant MWCNT retention at the low ionic strength, it is possible that non-physicochemical removal mechanisms are operative (e.g., straining).

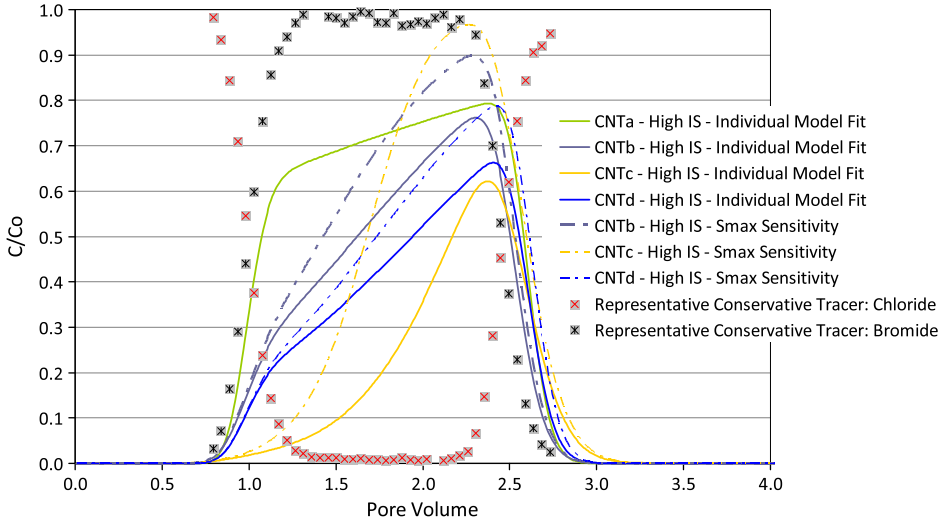

Fig. 3. Model breakthrough curves investigating sensitivity to S_{max} to initial injected MWCNT concentration. For the S_{max} sensitivity curves, S_{max} was scaled to the initial absorbance for the MWCNT-a experiment.

Table 4
Summary of Model Parameters when Fitted to MWCNT-a and b and MWCNT-c and d Together.

MWCNT	10 mmol/L Ionic strength experiments				0.1 mmol/L Ionic strength experiments			
	Attachment efficiency (α)	Maximum solid phase concentration (S_{max}) (μg/g)	Dispersivity (α_1) (m)	RMSE	Attachment efficiency (α)	Maximum solid phase concentration (S_{max}) (μg/g)	Dispersivity (α_1) (m)	RMSE
a and *b* (larger diameter)	9.24×10^{-2}	1.41	6.72×10^{-4}	1.24×10^{-1}	4.98×10^{-2}	1.30	2.27×10^{-3}	4.94×10^{-2}
c and *d* (smaller diameter)	2.10×10^{-1}	2.29	1.35×10^{-3}	9.82×10^{-2}	3.14×10^{-2}	2.29	1.39×10^{-3}	3.22×10^{-2}

While this modeling approach is based solely on CFT and a site blocking term, the inclusion of additional MWCNT removal mechanisms in the numerical simulator could further improve agreement between model and observed results. Additional experiments, however, would need to be conducted to evaluate the importance of any additional retention mechanisms. Another potential shortcoming in the model approach is the use of a collector efficiency that assumes monodispersed rod shaped MWCNTs [16]. MWCNTs likely aggregate to some extent in solution and are not rigid straight cylinders but instead, are often bent as indicated in the SEM micrographs (see Supplementary material). Furthermore, the collector efficiency only assumed traditional CFT retention processes (i.e., interception, sedimentation and diffusion), but additional retention processes may be necessary to describe the actual conditions and interactions present.

3.4. Summary and future work

Results from a series of column experiments suggest that smaller MWCNTs are retained to a greater extent in porous media than larger MWCNTs. Similarly, smaller MWCNTs have a greater number of retention sites available for deposition given that they can fit into smaller retention sites. This study also found that supplier provided MWCNT characteristics should be used with caution and independent characterization is typically warranted, a result in line with other studies [30–32]. Finally, an important finding is that the initial MWCNT mass is very important in the quantification model parameters. Initial MWCNT suspension concentrations were relatively high (i.e., ~mg/L) and would likely only be found close to MWCNT disposal sites. As such, it would probably require significantly more pore volumes of MWCNTs to observe breakthrough for lower and more environmentally relevant concentrations.

This study also raised a number of metrological issues that are important topics for future work related to nanoparticle and carbon nanotube transport in porous media. For example, the development of additional analytical techniques to quantify MWCNTs in addition to UV–Vis absorbance measurements is an important research topic. An additional orthogonal analytical technique would help increase the reliability of concentration measurements especially of the initial MWCNT solution. Currently, many scientists use the nominal concentration of MWCNTs in solution for their initial concentration assuming that all of the nanotubes added to the solution were suspended; one limitation to this approach revealed in a recent study is that MWCNTs typically may absorb substantial quantities of water depending upon their storage conditions [33]. Additionally, the development of standard methods for testing nanoparticle transport in porous media could help improve the reliability of reported transport results. Part of a standard method could include testing a reference nanoparticle such as the reference nanoparticle polystyrene beads available from the National Institute of Standards and Technology (NIST). This could highlight to what extent differences in observed transport behaviors stem from those among laboratories or among different scientists within a laboratory; in this study, such measurements may have helped clarify the differences between the results observed here and those by Mattison et al. [17] in addition to the expected differences as a result of the varying the aquatic chemistry conditions. Along these lines, inter-laboratory studies to identify and quantify sources of variability in these measurements could also help improve the reproducibility and reliability of nanoparticle transport studies. Lastly, characterizing the size distribution of MWCNTs was a significantly more challenging measurement than expected and methods for such measurements could be improved and standardized.

Acknowledgments

Certain commercial equipment or materials are identified in this paper in order to specify adequately the experimental procedure. Such identification does not imply recommendation or endorsement by the National Institute of Standards and Technology, nor does it imply that the materials or equipment identified are necessarily the best available for the purpose. Research performed in part at the NIST Center for Nanoscale Science and Technology. This research was supported by an Ontario Ministry of the Environment Best in Science Award, the Natural Sciences and Engineering Research Council of Canada and the Canadian Foundation for Innovation. The authors would like to thank Jeffrey Fagan for experimental advice and Ahmed I.A. Chowdhury for his experiments to assess quality control.

Appendix A. Supplementary material

Supplementary data associated with this article can be found, in the online version, at http://dx.doi.org/10.1016/j.jcis.2012.09.034.

References

[1] M.W. Shen, S.H. Wang, X.Y. Shi, X.S. Chen, Q.G. Huang, E.J. Petersen, R.A. Pinto, J.R. Baker, W.J. Weber Jr., J. Phys. Chem. C 113 (8) (2009) 3150–3156.
[2] X.Y. Shi, S.H. Wang, M.W. Shen, M.E. Antwerp, X.S. Chen, C. Li, E.J. Petersen, Q.G. Huang, W.J. Weber Jr., J.R. Baker, Biomacromolecules 10 (7) (2009) 1744–1750.
[3] J. Lee, S. Mahendra, P.J.J. Alvarez, ACS Nano 4 (7) (2010) 3580–3590.
[4] M.S. Mauter, M. Elimelech, Environ. Sci. Technol. 42 (16) (2008) 5843–5859.
[5] E.J. Petersen, L.W. Zhang, N.T. Mattison, D.M. O'Carroll, A.J. Whelton, N. Uddin, T. Nguyen, Q.G. Huang, T.B. Henry, R.D. Holbrook, K.L. Chen, Environ. Sci. Technol. 45 (23) (2011) 9837–9856.
[6] T. Galloway, C. Lewis, I. Dolciotti, B.D. Johnston, J. Moger, F. Regoli, Environ. Pollut. 158 (5) (2010) 1748–1755.
[7] E.J. Petersen, Q.G. Huang, W.J. Weber Jr., Environ. Sci. Technol. 42 (8) (2008) 3090–3095.
[8] E.J. Petersen, Q.G. Huang, W.J. Weber Jr., Environ. Health Perspect. 116 (4) (2008) 496–500.
[9] E.J. Petersen, Q.G. Huang, W.J. Weber Jr., Environ. Toxicol. Chem. 29 (5) (2010) 1106–1112.
[10] E.J. Petersen, R.A. Pinto, L. Zhang, Q.G. Huang, P.F. Landrum, W.J. Weber, Environ. Sci. Technol. 45 (8) (2011) 3718–3724.
[11] E.J. Petersen, J. Akkanen, J.V.K. Kukkonen, W.J. Weber Jr., Environ. Sci. Technol. 43 (8) (2009) 2969–2975.
[12] E.J. Petersen, R.A. Pinto, D.J. Mai, P.F. Landrum, W.J. Weber Jr., Environ. Sci. Technol. 45 (3) (2011) 1133–1138.
[13] Y.A. Tian, B. Gao, K.J. Ziegler, J. Hazard. Mater. 186 (2–3) (2011) 1766–1772.
[14] D.P. Jaisi, N.B. Saleh, R.E. Blake, M. Elimelech, Environ. Sci. Technol. 42 (22) (2008) 8317–8323.

[15] D.P. Jaisi, M. Elimelech, Environ. Sci. Technol. 43 (24) (2009) 9161–9166.
[16] X.Y. Liu, D.M. O'Carroll, E.J. Petersen, Q.G. Huang, C.L. Anderson, Environ. Sci. Technol. 43 (21) (2009) 8153–8158.
[17] N.M. Mattison, D.M. O'Carroll, R.K. Rowe, E.J. Petersen, Environ. Sci. Technol. 45 (22) (2011) 9765–9775.
[18] H.F. Lecoanet, J.Y. Bottero, M.R. Wiesner, Environ. Sci. Technol. 38 (19) (2004) 5164–5169.
[19] H.F. Lecoanet, M.R. Wiesner, Environ. Sci. Technol. 38 (16) (2004) 4377–4382.
[20] P. Wang, Q.H. Shi, H.J. Liang, D.W. Steuerman, G.D. Stucky, A.A. Keller, Small 4 (12) (2008) 2166–2170.
[21] Y.A. Tian, B. Gao, C. Silvera-Batista, K.J. Ziegler, J. Nanoparticle Res. 12 (7) (2010) 2371–2380.
[22] M. Elimelech, J. Gregory, X. Jia, R.A. Williams, Particle Deposition and Aggregation: Measurement, Modeling, and Simulation, Butterworth-Heinemann, Oxford, 1995. p 441.
[23] S.A. Bradford, S.R. Yates, M. Bettahar, J. Simunek, Water Resour. Res. 38 (12) (2002).
[24] N. Tufenkji, M. Elimelech, Langmuir 21 (3) (2005) 841–852.
[25] S.A. Bradford, J. Simunek, S.L. Walker, Water Resour. Res. 42 (2006) 1–12.
[26] J. Liu, A.G. Rinzler, H.J. Dai, J.H. Hafner, R.K. Bradley, P.J. Boul, A. Lu, T. Iverson, K. Shelimov, C.B. Huffman, F. Rodriguez-Macias, Y.S. Shon, T.R. Lee, D.T. Colbert, R.E. Smalley, Science 280 (5367) (1998) 1253–1256.
[27] K.M. Yao, M.M. Habibian, C.R. O'Melia, Environ. Sci. Technol. 5 (1971) 1105–1971.
[28] J.C. Lagarias, J.A. Reeds, M.H. Wright, P.E. Wright, SIAM J. on Opt. 9 (1) (1998) 112–147.
[29] N. Tufenkji, M. Elimelech, Langmuir 20 (25) (2004) 10818–10828.
[30] E.J. Petersen, B.C. Nelson, Anal. Bioanal. Chem. 398 (2) (2010) 613–650.
[31] D.B. Warheit, Toxicol. Sci. 101 (2) (2008) 183–185.
[32] H. Park, V.H. Grassian, Environ. Toxicol. Chem. 29 (3) (2010) 715–721.
[33] R.E. Sturgeon, J.W. Lam, A. Windust, P. Grinberg, R. Zeisler, R. Oflaz, R.L. Paul, B.E. Lang, J.A. Fagan, B. Simard, C.T. Kingston, Anal. Bioanal. Chem. 402 (1) (2012) 429–438.